

# Bimodal SegNet: Instance Segmentation Fusing Events and RGB Frames for Robotic Grasping

Sanket Kachole<sup>1</sup>, Xiaoqian Huang<sup>2</sup>, Fariborz Baghaei Naeini<sup>1</sup>, Rajkumar Muthusamy<sup>3</sup>, Dimitrios Makris<sup>1</sup> and Yahya Zweiri<sup>2</sup>

**Abstract**—Object segmentation for robotic grasping under dynamic conditions often faces challenges such as occlusion, low light conditions, motion blur and object size variance. To address these challenges, we propose a Deep Learning network that fuses two types of visual signals, event-based data and RGB frame data. The proposed Bimodal SegNet network has two distinct encoders, one for each signal input and a spatial pyramidal pooling with atrous convolutions. Encoders capture rich contextual information by pooling the concatenated features at different resolutions while the decoder obtains sharp object boundaries. The evaluation of the proposed method undertakes five unique image degradation challenges including occlusion, blur, brightness, trajectory and scale variance on the Event-based Segmentation (ESD) Dataset. The evaluation results show a 6-10% segmentation accuracy improvement over state-of-the-art methods in terms of mean intersection over the union and pixel accuracy. The model code is available at <https://github.com/sanket0707/Bimodal-SegNet.git>

**Index Terms**—Bimodal, Fusion, Segmentation, Robotics, Contours, Occlusion

## I. INTRODUCTION

Robotic grasping is the ability of the automated system to hold and manipulate target objects using the arm and end effectors. The grasping mechanism is mainly driven using sensors to locate the position and properties of the object for deploying advanced algorithms to control the movement of the robot's joints and fingers for a firm grasp [1]. It has wider industrial applications such as manufacturing plants, assembly lines, machining tasks and warehouses. An essential requirement to attempt a successful grasp include sensing, planning, control, adaptability and robustness. Vision-based robotic grasping methods including object detection, tracking, monitoring, inspection and gripping have delivered convincing results. These methods require a perception of the environment for the robot to execute the actions. Thus, the quality of the collected visual information is key to improving the performance in grasping applications [2].

\*This work was supported by Kingston University, the Advanced Research and Innovation Center (ARIC), and Khalifa University of Science and Technology, Abu Dhabi, UAE.

<sup>1</sup>Sanket Kachole, Fariborz Baghaei Naeini, and Dimitrios Makris are with Faculty of Science, Engineering and Computing, Kingston University, London, KT1 2EE. Corresponding author: K1742163@Kingston.ac.uk

<sup>2</sup>Xiaoqian Huang and Yahya Zweiri are with the Aerospace Engineering Department, Khalifa University of Science and Technology, Abu Dhabi, UAE. yahya.zweiri@ku.ac.ae

<sup>3</sup>Rajkumar Muthusamy is with Dubai Future Labs - RLab, Dubai, UAE rajkumar.muthusamy@dubaifuture.gov.ae

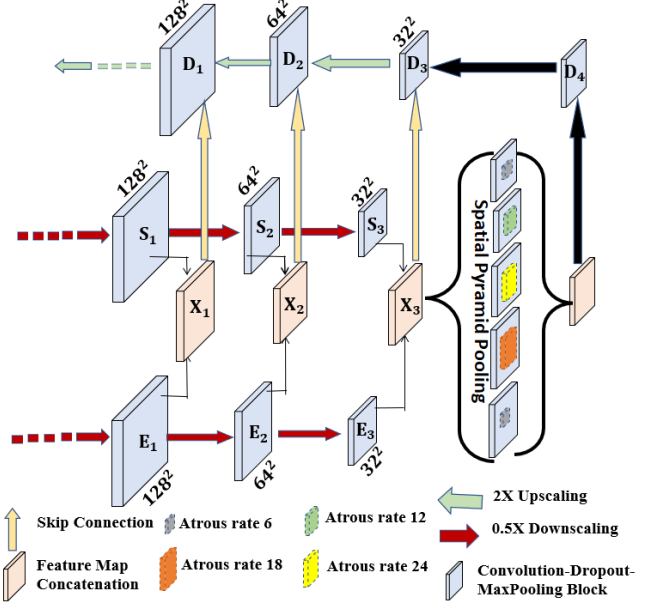


Fig. 1. Overview of the proposed Bimodal SegNet for robust object instance segmentation. The encoder-decoder-based architecture employs two separate encoders to handle the input from the RGB camera and the event camera. It further fuses the features using skip connections at multiple resolutions.

Although extensive efforts have been taken to deploy human-level grasping skills into robots [3], robotic grasps are still inferior to human ones. While grasping systems may operate under strict conditions (e.g. fix lighting, object type/size/orientation, etc), generalising their operation to a wider set of environmental settings is benefited by using visual sensors which provide richer and more detailed information regarding the object to be grasped, especially when combined with machine learning methods. In particular, object segmentation is relevant to robotic grasping, as they aim to extract the object boundaries at pixel level. Since visual information collected by cameras in the industrial environment may be affected by low light conditions, motion blur, object size variance, occlusion, etc [4], object segmentation methods should address such challenges.

Standard RGB cameras capture a full projection of the scene in sequences of frames. On the other side, neuromorphic cameras, a recent advance in visual sensors, record changes in pixel brightness as a stream of “events” [5]. Their advantage over standard RGB cameras is their high temporal resolution, low motion blur, low transmission bandwidth, high dynamic range

and low power. However, since events only record changes, their representative power is higher in textured regions and boundaries, but lower in uniform regions. [6], [7]. In addition, RGB cameras can capture contextual information and perform better when stationary and worse in high-speed due to motion blurring, while neuromorphic cameras are benefited by the camera motion that causes events to be generated around the object boundaries [8]. Both sensors are thus complementary and fusing their signals within a deep learning model may improve the accuracy of instance segmentation and address multiple challenges such as occlusion, blur, brightness and scale variance [9].

For this purpose, we introduce the Bimodal SegNet, a segmentation deep learning network that generalizes the traditional U-Net architecture [10] to handle asynchronous and irregular data from multiple sensors. The proposed network has two distinct encoders, one for each signal type, and a spatial pyramidal pooling with atrous convolutions [11] that capture rich contextual information by pooling the concatenated features at different resolutions while the decoder can obtain sharp object boundaries.

The main contribution of this paper are as follows:

- 1) We propose an encoder-decoder-based architecture that employs two separate encoders to handle the multimodal input by fusing the features with skip connections at multiple resolutions.
- 2) We demonstrate how to use atrous spatial pyramidal pooling within the context of bimodal encoder-decoder-based architecture in instance segmentation applications.
- 3) Our proposed model attains new state-of-the-art performance on ESD dataset [12] in terms of mean Intersection Over Union (mIoU) and Pixel Accuracy. Especially, it substantially outperforms the state-of-the-art methods under dark light conditions.

The rest of this paper is organized as follows. Section II reviews related works. The proposed architecture is described in detail in Section III. Section IV provides experimental results and an ablation study. Finally, Section V explains the conclusion and scope for further research.

## II. RELATED WORK

Instance segmentation aims to assign a separate class label to each object in an image [13]. Fully convolutional networks [14] introduced the idea of separating deep convolutional layers that perform feature extraction from the fully connected layers at the end of the architecture. The purpose of isolating the feature extraction blocks was to reuse classification networks like GoogleNet [15] and AlexNet [16] for other applications, using transfer learning. The loss of information due to the use of max pooling or dropout layers can be bypassed using skip connection by simply summing or concatenating the outputs of non-adjacent layers to avoid vanishing gradients. The concept of skip connections was applied on the U-Net architecture, which is based on encoder-decoder structure and applied in instance segmentation [10].

Robotic applications require techniques that achieve fine-grained pixel-level localization of class labels, especially in

critical applications such as robotic surgeries where few pixel errors could lead to undesired consequences [10] [17] [18]. The dilated convolution [19] also known as atrous convolution is a compelling convolutional tool that takes the features computed from the deep convolutional neural network and captures the context at various coarser resolutions by increasing the receptive fields convolution kernel. In other words, it is a method that expands the kernel size by inserting zeroes between its consecutive elements [20] [21] [22]. It also preserves detailed feature map resolutions without pooling or sub-sampling. Various models have been explored using atrous convolutions where experiments were performed by modifying atrous rates of capturing long-range information. Similarly, the application of combined U-Net with atrous convolution has been successfully implemented in [23] [24]. A convMixer-based UNet model is used in vision-based robotic grasping applications [25] which enhances the segmentation mask and boundary of unknown objects appearing in cluttered scenes.

Vision-based robotic grasping systems can be divided into mainly three types, depending on the sensors used: RGB-based, event-based and RGB-event fusion based. Traditional cameras capture visual information in the form of RGB frames continuously which leads to high power consumption. In addition, image quality may suffer e.g. blurring due to motion or low contrast in low lighting conditions which impact the segmentation and consequently the grasping quality [26] [27]. A recent study showed that traditional cameras are incompetent to capture blur-free movement on industrial conveyor belts due to a relatively low sampling rate, compared to event-based vision systems. Besides, the robotic gripper's actuating speed in industrial applications is a minimum of 100 ms [8] which also contributes to motion blur. Although high-speed frame-based cameras with a frame rate of more than 100 FPS are available, they demand higher power and storage consumption. Reducing latency is a significant consideration in robotic grasping applications. Complex algorithms in computer vision and image processing consume additional computing time which eventually impacts on overall grasping process [6]. This demands faster data acquirement and processing for efficient grasping. Lastly, improvement in data capturing processing and computation can reserve additional time for the gripper's actuation. Exploiting the advantage of high temporal resolution of events, [28] used the Xception encoder, supplied with 6 channels of image representation. The EV-SegNet [29] also used an Xception-based CNN to handle event data for semantic segmentation applications.

Various algorithms fuse modalities to take advantage of their complementarity. DAVIS produces events and frames simultaneously, making it a suitable visual sensor. CMX [30] employs a transformer-based architecture with a feature rectification module for semantic segmentation of cross-modality data. The recurrent architecture [9] has been explored to fuse the events and frames for depth prediction. The fusion of events and RGB frames has been successfully applied in simultaneous localization and mapping [31], high-dynamic range intensity reconstruction [32], feature tracking [28], and image deblurring [27]. However, none of them is applicable to the application of instance segmentation. Especially, in robotic

grasping applications where a dynamic environment increases the complexity to identify the accurate object contours and segment them to a sub-class level. In addition, existing methods lack showing generality to tackle frequently occurring issues in the factories for robotic grasping applications.

### III. BIMODAL SEGNET

In this section, the proposed Bimodal SegNet architecture for robust instance segmentation in robotic grasping applications is presented in details. Firstly, the conversion of asynchronous events into event frames is explained. Then, the concatenated skip connections between encoders and decoders are discussed. Next, the atrous convolution, which is the core element of the Spatial Pyramid Pooling is explained. Finally, the overall network architecture for the Bimodal SegNet is shown.

#### A. Event representation

The event stream generated from a dynamic vision sensor (DVS) is characterized by a position  $x_e$  and  $y_e$ , timestamp  $t_e$  and polarity  $p_e$  where  $e$  is the counter of events. The polarity is binary and thus either 0 for negative or 1 for positive polarity. In [33], the events were accumulated over a time window  $T$  irrespective of position information. In order to convert the asynchronous events into sequential frames, this paper uses the event accumulation method.

The configuration of the time window  $T$  hyperparameter should consider parameters such as the DVS threshold, application speed and noise, but most importantly the RGB frame rate. The event-to-frame conversion process can be formulated as:

$$E_t(x, y, p) = \sum_{\forall e} \text{rect}\left(\frac{t_e}{T} - 0.5 - t\right) \delta_{xx_e} \delta_{yy_e} \delta_{pp_e} \quad (1)$$

where  $E_t$  represents a frame of accumulated events for different polarities  $p \in \{0, 1\}$  at timestamp  $t$ . The Kronecker delta function and rectangle function are denoted as  $\delta$  and  $\text{rect}$  respectively. The  $t_e$  represents the timestamp of each event and  $e$  indicates the event number.

#### B. Concatenated Skip Connections

The concatenated skip connections maintain the information throughout the network as it allows connected layers to reuse the feature representation resulting in a performance improvement. As shown in Figure 2, the event encoder layers are from  $E_0$  to  $E_3$ . The standard encoder layers are from  $S_0$  to  $S_3$ . The decoder layers are  $D_0$  to  $D_3$ . Feature map from event encoders  $E_n$  is concatenated with feature map of standard encoder  $S_n$  as

$$X_n = ([E_n, S_n]) \quad (2)$$

where  $X_n$  represents the concatenated features with  $n$  ranges from 0 to 3. Further, the decoder layers receive the feature maps from the same level as the encoder and the previous decoder layer. It can be represented as,

$$D_n = ([X_n, D_{n+1}]) \quad (3)$$

The features extracted at various resolutions in the event encoders are bypassed to the same resolution of the standard encoder. The enriched features are then passed to the same resolution of the decoder.

#### C. Atrous convolution

Atrous convolution also called dilated convolution can be mathematically expressed as follows:

$$y[i] = \sum_{k=1}^K x[i + r.k] w[k] \quad (4)$$

where  $y$  is the output feature map and  $x$  is the input feature map.  $i$  represents the location in the output feature map  $y[i]$  in 2-D image. The convolution filter is stated by  $w$  and the atrous stride rate is determined by  $r$ . The atrous rate  $r$  increases the size of the kernel by inserting  $r - 1$  zeros along every spatial dimension. In the case of standard convolution, the value of rate is  $r = 1$ . The filter's receptive field is changed by modifying the stride rate [34].

#### D. Network Architecture for Bimodal SegNet

The architecture of the Bimodal SegNet Network is shown in Figure 2. Event-based vision sensors such as DAVIS346 can produce both continuous asynchronous events (with temporal resolution of few microseconds) and RGB frames (with frame rates between 25-50 Hz) simultaneously. The RGB frames are passed into RGB encoders  $S_n$  and the event frames are passed into event encoders  $E_n$ . Both types of encoders are built with convolutional blocks for downscaling the input frame by  $0.5x$  for  $N + 1$  consecutive times to learn or infer the feature maps. Event-based features mainly represent the object contours while RGB-based features provide rich contextual information.

At each of the  $N$  feature fusion stages in the encoder, a combination of convolution, dropout, convolution and MaxPooling layer is used. The output tensor of the convolution is passed into the dropout layer. It is further passed into the convolution layer and lastly into the MaxPooling layer to downsample the input along its spatial dimensions. The feature maps from the encoders are passed into multiple parallel atrous convolutional blocks with different sampling rates. The features extracted for each sampling rate within the spatial pyramidal pooling block are fused at the output of the block. The fused results are then passed into the decoder block where the image is upsampled by  $2x$  for  $N$  times consecutively. At each of the  $N$  feature fusion stages in the decoder, a combination of deconvolution, concatenation, convolution, dropout and convolution layer is used. The deconvolution layer assists in retrieving the original spatial dimension of the input image. Further, the concatenation layer takes the concatenated input tensor of the event encoder and RGB encoder i.e.  $X_n$  and output of the previous decoder layer i.e.  $D_{(n+1)}$  to provide a single fused tensor. The concatenated tensor is then passed into the dropout

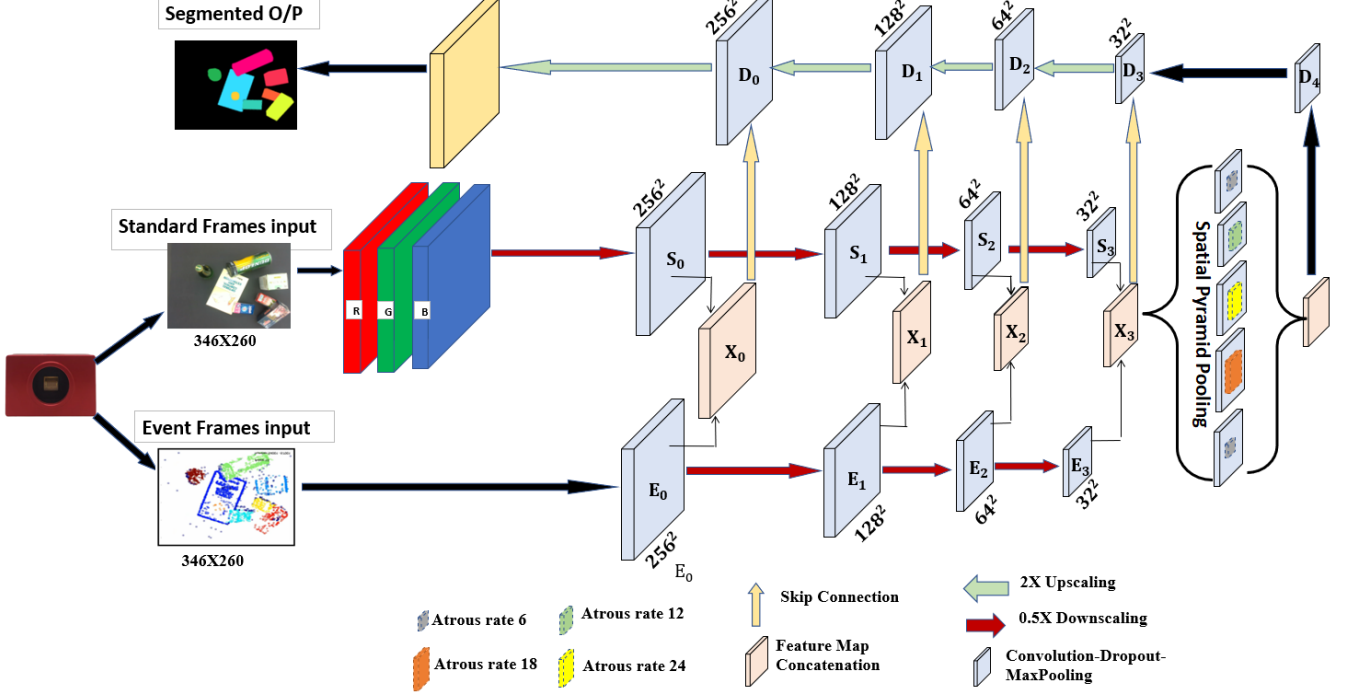


Fig. 2. Bimodal SegNet Architecture

layer to reduce the overfitting in the network and convolution. This allows the network to learn features at multiple scales, which is important to produce a scale-invariant model. Thus, the features from the event and RGB encoders are fused at each downscaling block and passed to the corresponding level of upscaling to the decoder block using a skip connection. The purpose of the concatenation in the decoder is to enrich the large-level features learned by the decoder block. Altogether, the network enriches the RGB frames at the decoder block by fusing the events frames and RGB frames at  $N$  separate feature resolutions and in the atrous spatial pyramid pooling block.

#### IV. EXPERIMENTATION

##### A. Dataset

ESD [12] is one of the largest datasets which focuses on instance understanding of robotic grasping scenes. The dataset was captured using the Davies346 sensor mounted on a robotic arm and consists of both conventional RGB frames and corresponding asynchronous events. In addition, the dataset has instance-wise dense pixel and events annotations for 15 classes grouped into 6 categories (bottle, box, pouch, book, mouse, platform). The dataset consists of 17186 annotated images and 177 labeled event streams. The captured dataset considers several variations such as in the camera's direction of motion, arm speed, lighting conditions and the number of objects in clutter. Motion variations are linear, rotational and partial-rotational motion. Arm speed variants are 0.15 m/s, 0.3 m/s and 1 m/s. Lighting conditions include normal light and low light. The number of objects in the clutter varies as 2,4,6,8,10 objects as shown in Table I. There are 13984 images

in the training dataset and 3202 images in the testing dataset. The five objects in the validation dataset are different from the testing dataset.

The RGB framerate is 40 Hz, therefore a temporal window of  $T=25$  ms is used for framing the events to ensure temporal alignment between the two types of frames. The RGB and event frame resolution is  $346 \times 260$ , which differs from the expected input of the network ( $256 \times 256$ ). Therefore, the popular approach of patchifying the input images is employed and the final segmentation map is reconstructed by unpatching the outputs.

##### B. Evaluation Metrics

1) **Pixel accuracy:** Pixel accuracy is a metric to calculate the percentage of pixels in the image that are classified correctly as given by Equation (5)

$$Acc(p, p') = \frac{1}{N} \sum_1^N \delta(p_i, p'_i) \quad (5)$$

where  $p, p'$ ,  $N$  and  $\delta$  represent the ground truth image, the predicted image, the total number of pixels and Kronecker delta function respectively. However, its descriptive power is limited in cases with a significant imbalance between foreground and background pixels.

2) **Mean Intersection over Union (mIoU):** The performance of the network for instance segmentation is evaluated using the mean Intersection over Union also known as the Jaccard Index. mIoU handles imbalanced binary and multi-class segmentation. It is calculated across classes according to Equation (6):

Raw Image	Ground Truth	Annotated Events
2 objects		
4 objects		
6 objects		
8 objects		
10 objects		

TABLE I

EXAMPLE OF THE ESD DATASET IN TERMS OF THE NUMBER OF OBJECTS ATTRIBUTES, UNDER THE CONDITION OF 0.15 MOVING SPEED, NORMAL LIGHT CONDITION, LINEAR MOVEMENT, AND 0.82 HEIGHT.

$$mIoU = \frac{1}{C} \sum_i^C \frac{\sum_i^N \delta(p_{i,c}, 1) \delta(p_{i,c}, p'_{i,c})}{\max(1, \delta(p_{i,c}, 1) + \delta(p'_{i,c}, 1))} \quad (6)$$

Thus, the mIoU measure is more informative than the pixel accuracy as it considers false positives.

### C. Training

The RestNet-101 pretrained on ImageNet is the backbone of the model that is treated as an encoder to extract features. The last layer of the pretrained ResNet-101 is replaced with 11 instance classes (10 objects and 1 background). The whole dataset is divided into training/testing/validation with a ratio of 70:20:10. The number of filters in the event/RGB encoders at  $E_0/S_0$ ,  $E_1/S_1$ ,  $E_2/S_2$ ,  $E_3/S_3$  are 16, 32, 64, 128 respectively. The kernel size of the convolution layer is 3. The output tensor convolution is passed into the dropout layer where the input units are randomly set to 0 with a frequency of 0.2 in order to avoid overfitting. The MaxPooling layer is  $2 \times 2$  in size to take the maximum value over each channel of the input window. Using empirical results [11], typically 6, 12, 18, 24 atrous rate for RGB and 6 atrous rate for event frames are used. Since the event frames have mainly edge-level information, the use of atrous rate  $r = 6$  assists in preventing information leak at this stage. A  $3 \times 3$  kernel size for convolution is empirically selected as it is small enough to capture local spatial information. Softmax as an activation function and Adam as an optimizer are used while compiling

the model. Categorical cross-entropy is used as a loss function. The fine-tuned model has 0.001 learning rate, 30 batch size, 100 epochs. The training was performed on a processor 11th Gen Intel(R) Core(TM) i7-1165G7, 1.69 GHz and 16 GB RAM.

### D. Alternative Architectures for Ablation studies

To demonstrate the validity of the proposed architecture, we investigate alternative approaches that vary at the stage where the fusion of RGB and events frames occurs and its impact on segmentation accuracy. The following two architectures are considered:

1) **Pre-Encoder Fusion:** The pre-encoder fusion architecture is derived from U-Net architecture where event and RGB frames are concatenated and passed into the single encoder and its output is passed into the decoder, without any skip connections or atrous convolutions (Figure 3).

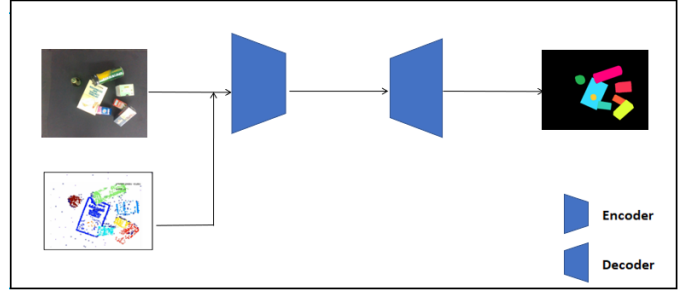


Fig. 3. Pre-Encoder Fusion Architecture: RGB and event frames are fused before encoding. The architecture lacks any skip connections and atrous convolutions

2) **Pre-Decoder Fusion:** In the Pre-Decoder fusion approach, event and RGB frames are encoded separately similar to the proposed model, except the skip connections between encoders and the decoder as shown in Figure 2. Instead, the low-dimension outputs of the two encoders are concatenated and fed into a single decoder. The Spatial Pyramid Pooling is also omitted (Figure 4).

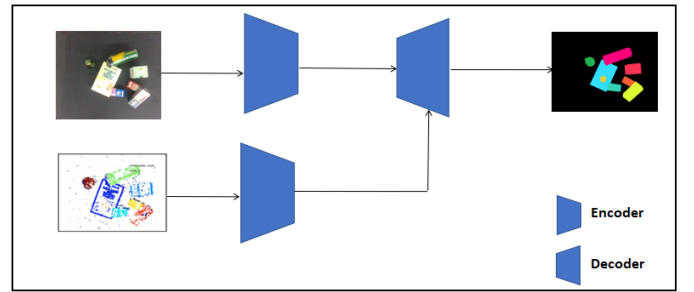


Fig. 4. Pre-Decoder Fusion Architecture: RGB and event frames are encoded separately and fused before decoding. The architecture lacks any skip connections and atrous convolutions

### E. Results

To assess model robustness, experiments were conducted, varying object clutter, lighting, camera distance, trajectory,

and speed. The proposed model was compared to state-of-the-art models, including RGB-based FCN [14], U-Net [10], DeepLab [11], RGB-event fusion CMX [30] and models in the ablation study in subsection IV-D. In addition, the CMX model used in this study is trained on the ESD dataset [12] using default parameters for feature fusion of multiple modalities described in [30]. If not explicitly specified, the following default conditions will be considered to define the testing subsets for the experiments: 2 objects, normal light, rotational arm motion, 0.15 m/s speed and 62 cm platform to camera distance. Evaluation metrics, ablation study, and results are discussed below.

**1) Varying objects/occlusion using pre-trained ResNet-101 encoder:** The first experiment was conducted on a subset of the testing dataset where the number of objects in the clutter varied between 2,4,6,8,10. The scenario of two objects indicates no occlusion, while in scenarios of more than 2 objects occlusions are present. Moreover, the higher the number of objects, the more occlusion and the higher complexity in the scenario. This is also evident in the segmentation accuracy results of all models, as shown in Figure 5, where the mIoU score of all models is decreasing with the increasing number of objects. The mIoU score for all the state-of-the-art models for 2 objects ranges from 54.65% to 92.46% and it drops for 10 objects (38.42% to 85.42%). whereas, the proposed Bimodal SegNet model's performance drops only by 7.97% and maintains better performance than the other methods, including state-of-the-art models such as FCN, U-Net and DeepLab, pre-trained on ImageNet for any number of scene objects.

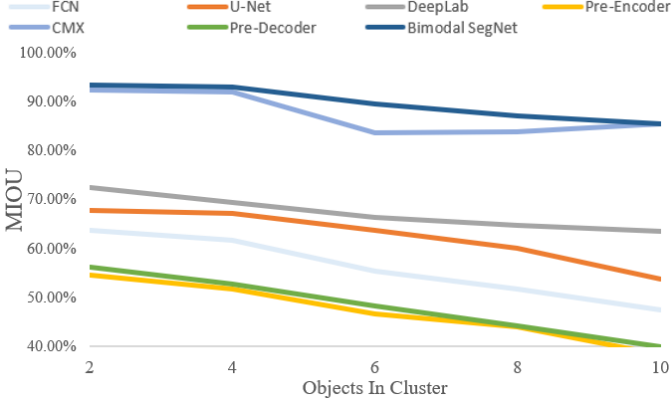


Fig. 5. Segmentation accuracy of the pre-trained encoder in varying clutter objects scene

**2) Varying objects/occlusion using re-trained encoders:** In order to tackle the challenge of substantial loss in accuracy for 10 objects in clutter, transfer learning is employed by unfreezing the last 4 convolution layers of the encoder, the whole decoder module, and the classifier of the ResNet-101 on the similar data used in experiment IV-E1. Figure 6 shows that this certainly improves the overall accuracy of all the models. As far as FCN, U-Net and DeepLab are concerned, the average accuracy increased by about 7% for all scenarios. The proposed Bimodal SegNet model still maintains the highest

mIoU score, e.g 95.46% for the 2-object scenario and with a drop of only 7.97% for the 10-object scenario.

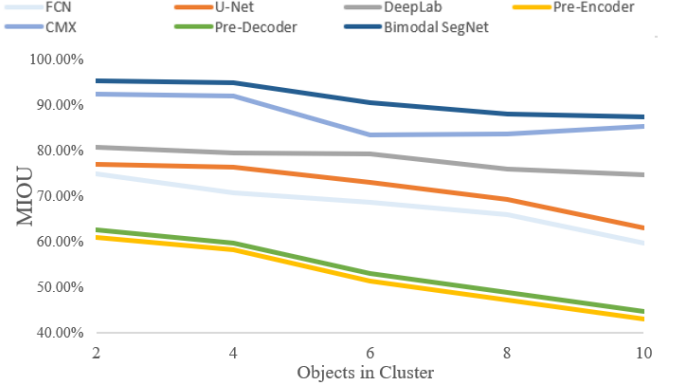


Fig. 6. Segmentation accuracy of re-trained encoder in varying clutter objects scene

**3) Varying lighting conditions using re-trained encoder:** State-of-the-art RGB-based methods struggle in low light conditions, as objects are not clearly visible. This is reflected on the huge drop in their segmentation accuracy between bright and low conditions, as shown in Figure 7: 34.9%, 32.08% and 31.55% for FCN, U-Net and DeepLab respectively. Methods that fuse RGB and event frames demonstrate some resilience in low light conditions, with smaller drops in segmentation accuracy: 5.85%, 7.04%, and 2.13% for the Pre-Encoder Architecture, the Pre-Decoder Architecture and the CMX respectively. The proposed Bimodal SegNet seems to be robust against varying lighting conditions with the lowest drop of only 1.60% in segmentation accuracy.

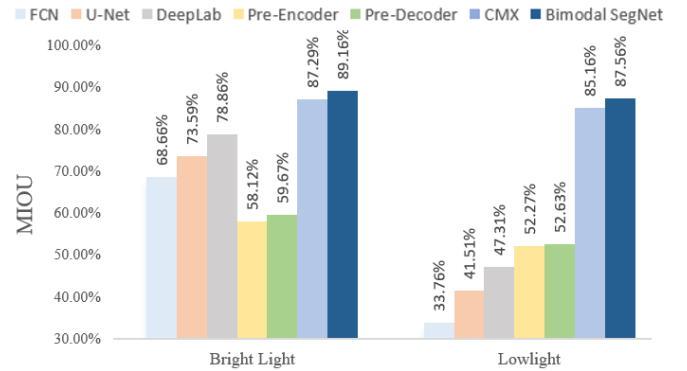


Fig. 7. Segmentation accuracy in varying lighting conditions scene

**4) Varying moving trajectories using re-trained encoder:** The subsequent experiment was conducted on a subset of the testing dataset, where the robotic arm movement direction was varied as linear, rotational, or partial rotational. In event-based vision sensors, the direction of the robotic arm movement plays a crucial role as perpendicular edges generate more informative event sets compared to parallel edges. However, linear motion is marked by abrupt directional changes while rotational motion involves smoother curves, causing higher jerk and vibrations in linear motion, leading to more blurred images than in rotational and partial rotational motion. The

impact of the phenomenon is demonstrated in Figure 8, where FCN, U-Net, and DeepLab models were evaluated on RGB images. Their average mIoU score is highest in rotational motion 67.74%, decreasing by 4.65% in partial rotational and 10.95% in linear motion. Methods that combine RGB and event frames are proved more robust with smaller drops. The proposed Bimodal Segnet maintains its superiority in segmentation accuracy, but also demonstrates the lowest variation across different motion directions.

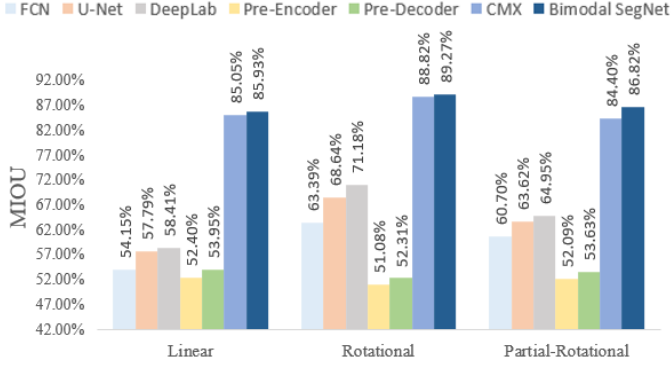


Fig. 8. Segmentation accuracy in varying directions of robotic arm motion scene

5) **Moving speed of camera using re-trained encoder:** The camera is placed at the end of the robotic arm thus the camera speed and resultant blur in images is an important factor while evaluating the robustness of the model. This experiment was conducted on a subset of the training dataset where the speed of the end effector was varied. State-of-the-art models have an mIoU score ranging from 64.89% to 86.58% for 0.15 m/s which then drops to a range of 46.45% to 84.90% for 1m/s (Figure 9). Whereas, the proposed Bimodal SegNet model has the highest accuracy of 89.31% for 0.15m/s and it drops to 86.72% for 1m/s i.e. by 2.59%. The impact of event-based vision in high-speed conditions is clear as it assists in the accurate estimation of contours.

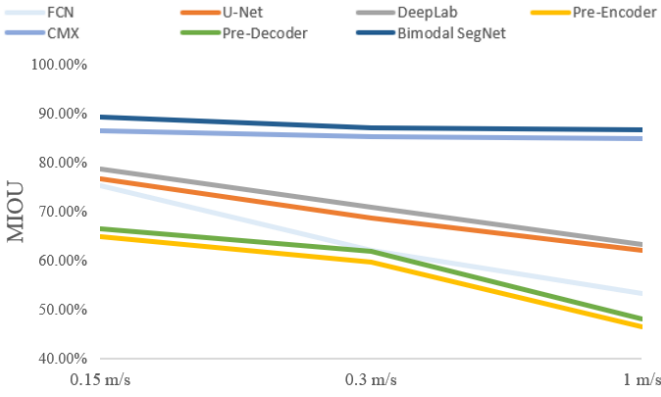


Fig. 9. Segmentation accuracy in varying speed of robotic arm

6) **Object size variance using re-trained encoder:** In order to understand the scale invariance of the model the experiment was conducted on a subset of the training dataset where the distance between the platform and the camera was varied to 62

cm and 82 cm. As per the results illustrated in figure 10 there is a minimal impact of the camera and object distance on the accuracy of all the models, yet, a drop in performance of the Bimodal SegNet is only 0.37% ie. from 86.53% to 86.16% as compared to the state of the art models i.e. 3.17% ie. 71.24% to 68.07%.

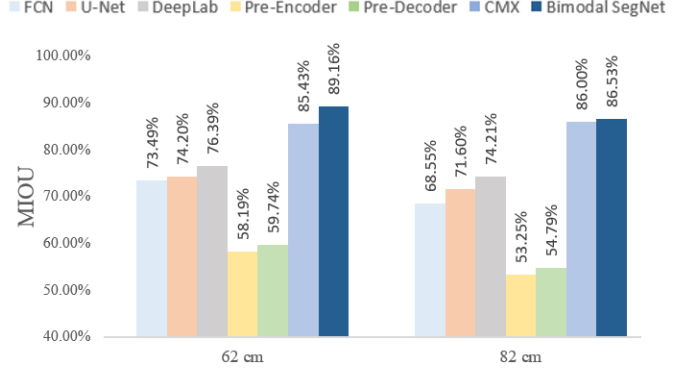


Fig. 10. Segmentation accuracy in varying distance between object and camera scene

Method	mIoU	Pixel Accuracy
FCN [14]	59.6	70.48
U-Net [10]	64.7	75.2
DeepLab [11]	71.05	81.06
Pre-Encoder [IV-D1]	51.3	72.2
Pre-Decoder [IV-D2]	52.7	73.1
CMX [30]	85.81	94.58
Bimodal SegNet [ours]	<b>87.05</b>	<b>96.83</b>

TABLE II

QUANTITATIVE COMPARISON OF BIMODAL SEGNET AGAINST OTHER RGB-BASED AND RGB-EVENT FUSION METHODS ON THE WHOLE ESD DATASET.

7) **Quantitative Comparison:** Segmentation results of the FCN, U-Net, DeepLab, Pre-Encoder, Pre-Decoder, CMX and Bimodal SegNet on the whole testing part of the ESD dataset, i.e. considering all possible variations of object numbers, lighting conditions, motion type and speed, as well as distance from the camera, are shown in the Table II using the pixel accuracy and the mIoU metrics. The proposed Bimodal SegNet outperforms the traditional RGB-based methods demonstrating the value of fusing RGB and event frames. In addition, it outperforms all other architectures that fuse RGB and event frames, including the state-of-the-art CMX [30], illustrating the superiority of the proposed architecture. The CMX architecture achieves 85.81% mIoU and 94.58% pixel accuracy, still these scores are 1.24% and 2.25% respectively lower than what is achieved by the proposed Bimodal SegNet model.

## V. CONCLUSIONS

In this paper, a novel architecture for instance segmentation in robotic grasping using a dynamic vision sensor is presented. The architecture fuses the event frames and RGB frames at various resolutions of the event encoder and RGB encoder, which further fuses the feature maps in the decoder. The feature maps from both encoders are passed into the spatial pyramidal block where atrous convolutions are employed.

Our proposed model achieves state-of-the-art performance on the ESD dataset in terms of mIoU and pixel accuracy, as demonstrated in multiple scenarios with variations in object types, trajectory, camera speed, apparent size, and lighting conditions. The fusion approach we propose achieves high robustness against various challenges, such as occlusions, low lighting, small objects, high speed, and linear motion. Bimodal SegNet, leveraging the complementarity of events and frames, outperforms unimodal encoder-decoder approaches. The experimental comparisons to alternative fusion strategies, including the state-of-the-art transformer-based CMX, demonstrate the superiority of our proposed architecture that fuses RGB and event frames at multiple resolutions, with skip connections and atrous convolutions.

Our future objective is to improve the current method's temporal limitations caused by event framing by incorporating an asynchronous event-based approach to effectively leverage the event camera's high temporal resolution for unknown object segmentation.

## REFERENCES

- [1] V. P. Dinakaran, M. P. Balasubramaniyan, Q. H. Le, A. J. Alrubaie, A. Al-khaykan, S. Muthusamy, H. Panchal, M. M. Jaber, A. K. Dixit, and C. Prakash, "A novel multi objective constraints based industrial gripper design with optimized stiffness for object grasping," *Robotics and Autonomous Systems*, vol. 160, 2023.
- [2] G. Du, K. Wang, S. Lian, and K. Zhao, "Vision-based robotic grasping from object localization, object pose estimation to grasp estimation for parallel grippers: a review," *Artificial Intelligence Review*, vol. 54, no. 3, pp. 1677–1734, 2021.
- [3] K. Sanket, M. Manish, and B. Anurag, "3 Dimensional Welding SPM/Path Tracker," *International Journal Of Design And Manufacturing Technology*, vol. 7, no. 3, 12 2016.
- [4] F. Bader and S. Rahimifard, "Challenges for industrial robot applications in food manufacturing," in *ACM International Conference Proceeding Series*. Association for Computing Machinery, 2018.
- [5] F. Liao, F. Zhou, and Y. Chai, "Neuromorphic vision sensors: Principle, progress and perspectives," *Journal of Semiconductors*, vol. 42, no. 1, 2021.
- [6] X. Huang, R. Muthusamy, E. Hassan, Z. Niu, L. Seneviratne, D. Gan, and Y. Zweiri, "Neuromorphic vision based contact-level classification in robotic grasping applications," *Sensors (Switzerland)*, vol. 20, no. 17, pp. 1–15, 2020.
- [7] R. Muthusamy, A. Ayyad, M. Halwani, D. Swart, D. Gan, L. Seneviratne, and Y. Zweiri, "Neuromorphic Eye-in-Hand Visual Servoing," *IEEE Access*, vol. 9, pp. 55 853–55 870, 2021.
- [8] R. Muthusamy, X. Huang, Y. Zweiri, L. Seneviratne, and D. Gan, "Neuromorphic Event-Based Slip Detection and Suppression in Robotic Grasping and Manipulation," *IEEE Access*, vol. 8, pp. 153 364–153 384, 2020.
- [9] D. Gehrig, M. Ruegg, M. Gehrig, J. Hidalgo-Carrio, and D. Scaramuzza, "Combining Events and Frames Using Recurrent Asynchronous Multi-modal Networks for Monocular Depth Prediction," *IEEE Robotics and Automation Letters*, vol. 6, no. 2, pp. 2822–2829, 2021.
- [10] O. Ronneberger, P. Fischer, and T. Brox, "U-net: Convolutional networks for biomedical image segmentation," vol. 9351. Springer Verlag, 2015, pp. 234–241.
- [11] L. C. Chen, Y. Zhu, G. Papandreou, F. Schroff, and H. Adam, "Encoder-decoder with atrous separable convolution for semantic image segmentation," vol. 11211 LNCS. Springer Verlag, 2018, pp. 833–851.
- [12] X. Huang, K. Sanket, A. Ayyad, F. B. Naeini, D. Makris, and Y. Zweiri, "A Neuromorphic Dataset for Object Segmentation in Indoor Cluttered Environment," 2 2023. [Online]. Available: [https://kuacae-my.sharepoint.com/personal/100049863\\_ku\\_ac\\_ae/\\_layouts/15/onedrive.aspx?id=%2Fpersonal%2F100049863%5Fku%5Fac%5Fae%2FDocuments%2FESD&ga=1](https://kuacae-my.sharepoint.com/personal/100049863_ku_ac_ae/_layouts/15/onedrive.aspx?id=%2Fpersonal%2F100049863%5Fku%5Fac%5Fae%2FDocuments%2FESD&ga=1)
- [13] C. Xie, Y. Xiang, A. Mousavian, and D. Fox, "Unseen Object Instance Segmentation for Robotic Environments," *IEEE Transaction on Robotics*, 2020.
- [14] J. Long, E. Shelhamer, and T. Darrell, "Fully convolutional networks for semantic segmentation," *Computer Vision and Pattern Recognition*, pp. 431–440, 2015.
- [15] C. Szegedy, W. Liu, Y. Jia, P. Sermanet, S. Reed, D. Anguelov, D. Erhan, V. Vanhoucke, and A. Rabinovich, "Going Deeper with Convolutions," *CVPR*, 2014.
- [16] A. Krizhevsky, I. Sutskever, and G. E. Hinton, "ImageNet Classification with Deep Convolutional Neural Networks," *NeuralIPS*, 2012.
- [17] N. Nathoo, M. C. Çavuşoğlu, M. A. Vogelbaum, and G. H. Barnett, "In touch with robotics: Neurosurgery for the future," pp. 421–431, 3 2005.
- [18] C. Y. Lin, Y. C. Chiu, H. F. Ng, T. K. Shih, and K. H. Lin, "Global-and-local context network for semantic segmentation of street view images," *Sensors (Switzerland)*, vol. 20, no. 10, 5 2020.
- [19] L.-C. Chen, G. Papandreou, F. Schroff, and H. Adam, "Rethinking Atrous Convolution for Semantic Image Segmentation," 2017.
- [20] F. Yu and V. Koltun, "Multi-Scale Context Aggregation by Dilated Convolutions," 11 2015.
- [21] L.-C. Chen, G. Papandreou, I. Kokkinos, K. Murphy, and A. L. Yuille, "Semantic Image Segmentation with Deep Convolutional Nets and Fully Connected CRFs," *IEEE Transactions on Pattern Analysis and Machine Intelligence*, 2014.
- [22] L. C. Chen, G. Papandreou, I. Kokkinos, K. Murphy, and A. L. Yuille, "DeepLab: Semantic Image Segmentation with Deep Convolutional Nets, Atrous Convolution, and Fully Connected CRFs," *IEEE Transactions on Pattern Analysis and Machine Intelligence*, vol. 40, no. 4, pp. 834–848, 2018.
- [23] S. Safarov and T. K. Whangbo, "A-denseunet: Adaptive densely connected unet for polyp segmentation in colonoscopy images with atrous convolution," *Sensors*, vol. 21, no. 4, pp. 1–15, 2021.
- [24] Y. Lv, H. Ma, J. Li, and S. Liu, "Attention Guided U-Net with Atrous Convolution for Accurate Retinal Vessels Segmentation," *IEEE Access*, vol. 8, pp. 32 826–32 839, 2020.
- [25] X. Huang, R. Azzam, S. Javed, D. Gan, L. Seneviratne, A. Abusafieh, and Y. Zweiri, "CM-UNet: ConvMixer UNet for Segmentation of Unknown Objects in Cluttered Scenes," *IEEE Access*, 2022.
- [26] T. Brooks, J. T. Barron, and G. Research, "Learning to Synthesize Motion Blur," *CVPR*, 2019.
- [27] Liyuan Pan, "Bringing a Blurry Frame Alive at High Frame-Rate with an Event Camera," *CVPR*, 2019.
- [28] D. Gehrig, H. Rebecq, G. Gallego, and D. Scaramuzza, "Asynchronous, Photometric Feature Tracking using Events and Frames," *ECCV*, 2018.
- [29] I. Alonso and A. C. Murillo, "EV-SegNet: Semantic Segmentation for Event-based Cameras," *IEEE/CVF Conference on Computer Vision and Pattern Recognition Workshops*, 2018.
- [30] H. Liu, J. Zhang, K. Yang, X. Hu, and R. Stiefelhagen, "CMX: Cross-Modal Fusion for RGB-X Semantic Segmentation with Transformers," 2022.
- [31] A. Z. Zhu, L. Yuan, K. Chaney, and K. Daniilidis, "Unsupervised Event-based Learning of Optical Flow, Depth, and Egomotion," *CVPRW*, 12 2018.
- [32] A. Tomy, A. Paigwar, K. Singh Mann, A. Renzaglia, C. Laugier, and K. S. Mann, "Fusing Event-based and RGB camera for Robust Object Detection in Adverse Conditions," *HAL Open Science*, 2017.
- [33] F. B. Naeini, D. Makris, D. Gan, and Y. Zweiri, "Dynamic-vision-based force measurements using convolutional recurrent neural networks," *Sensors (Switzerland)*, vol. 20, no. 16, pp. 1–15, 8 2020.
- [34] L. C. Chen, Y. Zhu, G. Papandreou, F. Schroff, and H. Adam, "Encoder-decoder with atrous separable convolution for semantic image segmentation," in *Lecture Notes in Computer Science*, vol. 11211 LNCS. Springer Verlag, 2018, pp. 833–851.